Journal of Hazardous Materials 182 (2010) 408–415

Contents lists available at ScienceDirect

Journal of Hazardous Materials

journal homepage: www.elsevier.com/locate/jhazmat

Adsorption kinetic character of copper ions onto a modified chitosan transparent thin membrane from aqueous solution

Zihong Cheng, Xiaoshuai Liu, Mei Han, Wei Ma*

Research Centre of Seawater Desalination and Multipurpose Utilization, Department of Chemistry, Dalian University of Technology, Dalian 116023, PR China

ARTICLE INFO

Article history:
Received 31 December 2009
Received in revised form 1 June 2010
Accepted 14 June 2010
Available online 18 June 2010

Keywords:
Chitosan
Adsorptive membrane
Copper ions
Adsorption kinetics

ABSTRACT

A modified chitosan transparent thin membrane (MCTTM) was prepared and used as the adsorbent to investigate the adsorption kinetics due to excellent capacity of removing copper ions in water solution. The structure and morphology of MCTTM were characterized by SEM analysis and FTIR analysis. External mass transfer, intra particle diffusion, and pseudo-first and pseudo-second order models were used to describe the adsorption process. The results obtained from the study illustrated that the adsorption process could be described by the pseudo-second order model, which indicated adsorption process was a chemical adsorption behavior of chelation ion exchange proved by the FTIR and adsorption free energy analysis. External mass transfer and intra particle diffusion processes were the rate-controlling steps.

1. Introduction

The increasing contamination of urban and industrial wastewater by heavy metal ions is a worrying environmental problem because of its toxic effect to plants, animals and human beings. Unlike the organic wastes, these inorganic pollutants are of considerable concern because they are non-biodegradable, accumulated in living tissues, highly toxic to cause various diseases and disorders, and have a probable carcinogenic effect [1,2]. Copper is an essential micronutrient, vital for the body in small quantity, but at high amounts (over 1.3 mg L^{-1}) [3], it has been reported to cause stomach and intestine problems, neurotoxicity, jaundice, and liver toxicity [4]. Moreover, continued inhalation of copper-containing sprays is linked with an increase in lung cancer among exposed workers [5]. This has motivated many studies during the past several years toward the development of new processes for the treatment of containing copper ions effluents. Conventional techniques used for removal of heavy metal ions from aqueous effluents, such as chemical precipitation, ion exchange, electrodialysis, solvent extraction, membrane separation, have been found limited as some are incapable of reducing the concentration to the required levels and often involve high capital and operational cost and some may also generate secondary wastes which present treatment problems, such as the large quantity of sludge generated by precipitation processes [6,7]. Adsorption is a physicochemical treatment process found effective in removing heavy metal ions from wastewater [2]. Low-cost adsorbent required little processing, abundant in nature, or from by-products and waste materials from other industries is available [8].

Some studies focus on adsorptive membranes to remove heavy metal ions from aqueous solutions. These membranes have reactive functional groups on the membrane surface, including –COOH, $–SO_3H$, and $–NH_2$ groups, which could bond with heavy metal ions by forming surface complexation or ion exchange mechanisms [9]. Heavy metal ions can be removed when the ions are in contact with the surface of the membrane, even when the pore sizes of the membrane are much lager than the dimensions of the metal ions. Adsorptive adsorbents prepared by polymer chitosan (CS) have attracted obvious attentions in biomedical or biochemical field for separation and purification, and in the environmental field for the removal of heavy metal ions, such as the removal of protein [4,10], the removal of dyestuffs [11,12], and adsorption of heavy metal ions [3,9,13–16]. Chitosan is a heteropolymer with high content of amine ($–NH_2$) functional group and remarkable availability. It is composed of both glucosamine and acetyglucosamine units and produced by the alkaline deacetylation of chitin presented in insect cuticles and crustacean shells [4,11,17]. However, there are few literatures found to prepare chitosan transparent thin adsorptive membrane to remove lower concentrations of copper ions in the solution. Previous work of this study has reported a novel modified chitosan transparent thin membrane which presents capacity to remove copper ions of lower concentrations by adsorption and performances to test heavy metal ions by color changing [18].

* Corresponding author. Tel.: +86 411 8470 6303; fax: +86 411 8470 7416.
E-mail addresses: chmawv@yahoo.com, mawei@dlut.edu.cn (W. Ma).

0304-3894/$ – see front matter.
doi:10.1016/j.jhazmat.2010.06.048

Nomenclature

a_m	specific area of the MCTTM ($m^2\ m^{-3}$)
c	concentration of copper ions at equilibrium ($mg\ L^{-1}$)
c_0	concentration of copper ions at initial ($mg\ L^{-1}$)
c_s	solute concentration at the surface of adsorbent ($mg\ L^{-1}$)
C	intercept ($mg\ g^{-1}$)
C_e	equilibrium concentration ($mol\ m^{-3}$)
E	adsorption free energy ($kJ\ mol^{-1}$)
E_a	Arhenius activation energy ($J\ mol^{-1}$)
k_0	frequency factor ($g\ h\ mg^{-1}$)
k_1	rate constant of the pseudo-first order model (h^{-1})
k_2	rate constant of the pseudo-second order equation ($g\ h\ mg^{-1}$)
k_f	mass transfer coefficient between bulk solution and solid surface ($m\ h^{-1}$)
k_V	equation rate constant ($(mg\ g^{-1})^2\ h^{-1}$)
k_{WM}	intra particle diffusion rate constant of Weber and Morris ($h^{-1/2}$)
m	mass of the MCTTM added during adsorption process (g)
q	adsorption amount per mass MCTTM ($mg\ g^{-1}$)
q_i	estimated from the kinetic for corresponding Q_i ($mg\ g^{-1}$)
Q	adsorption capacity at equilibrium ($mol\ kg^{-1}$)
Q_i	observation from the experiments ($mg\ g^{-1}$)
Q_{max}	maximum amount per unit mass of the MCTTM ($mol\ kg^{-1}$)
R	universal gas constant $8.314 \times 10^{-3}\ kJ\ mol^{-1}\ K^{-1}$
t	adsorption time (h)
T	temperature (K)
T_1	temperature 298 K
V	volume of solution (L)
β	activity coefficient ($mol^2\ kJ^{-2}$)

The objectives of this study are to characterize the modified chitosan transparent thin membrane (MCTTM) by SEM, FTIR and pH_{pzc} analysis; to investigate the effect of the MCTTM thickness, the kinetics characteristics and the Arhenius activation energy of the adsorption process; to discuss the adsorption mechanism of adsorption copper ions from the aqueous solution with lower concentrations by the MCTTM finally.

2. Experimental

2.1. Reagents and instrumentations

Chitosan (CS) with 92.9% deacetylation degree was provided by Qingdao Yunzhou Biochemistry Co., Ltd. (China). Copper nitrate trihydrate, supplied by Kermel, Tianjin, was used to prepare copper ions solution in the adsorption experiments. Sodium hydroxide supplied by Shenyang (China), acetic acid, sodium nitrate and nitric acid were purchased from Dalian (China). All the reagents were of analytical grade.

A flame atomic absorption spectrophotometer (SOLAN969 Model, USA) was employed for determination of copper ions. An acidimeter (PHS-2 Model, Hang Zhou, China) was used to measure pH of solutions. The structure and morphology of the prepared membrane were examined by SEM (JEOL JMS-5600LV) and FTIR (Bruker TENSOR 27 FTIR) analysis.

Table 1
The physical and chemical characters of the MCTTM.

	Characters of the MCTTM	Characterization
Thickness	About 10 μm	SEM analysis
Structure	Homogeneous porous structure	SEM analysis
pH_{pzc}	7.8	pH_{pzc} analysis
WSR (water swelling ratio)	126%	WSR analysis [18]
Chemical groups	–OH and $–NH_2$ group	FTIR analysis

2.2. Synthesis and characterization

The modified chitosan transparent thin membrane (MCTTM) was prepared by solution casting method [18]. Chitosan acetic acid solution was obtained by dissolving 1.5 g chitosan powder in 100 mL 2% acetic acid solution stirred by a magnetic stirrer. 1 g polyvinylalcohol was dissolved in 30 mL deionized water by heating to make a cross-linking solution. Then, the above two solutions were mixed together by mechanical stirring in definite proportions to prepare homogeneous membrane casting dope solution. Thereafter, the resultant solution was left in the beaker without stirring for 48 h at 50 °C to sufficiently free the air bubbles and cross-link. Afterwards, the solution was cast on a rimmed glass plate and dried at room temperature. The dried membrane was immersed in diluted sodium hydroxide solution to free the membrane and neutralize the excess acid, and then the membrane was washed exhaustively with deionized water until all alkali was removed. Lastly, the membrane was dried at room temperature and stored. The MCTTM was characterized by SEM and FTIR analysis.

Batch equilibration technique was applied to determine pH at the point of zero charge (pH_{pzc}) [19]. $NaNO_3$ was used as the electrolyte and the ionic strength was kept constant in all experiments. 0.1 g of MCTTM was introduced into 50 mL of 0.5 mol L^{-1} and 0.01 mol L^{-1} $NaNO_3$ solution respectively. Initial pH values of $NaNO_3$ solutions were adjusted from about 2 to 12 by diluted HNO_3 or NaOH. The mixtures were allowed to equilibrate for 24 h in a shaker thermostated at 20 °C. Then the mixtures were separated and the final pH values (pH_{final}) were measured again. The pH_{pzc} of the MCTTM was determined from the plots ΔpH ($pH_{final}–pH_{initial}$) versus $pH_{initial}$.

The physical and chemical characters of the MCTTM were shown in Table 1.

2.3. Effect of membrane thickness on the adsorption capacity

To examine the effect of thickness of MCTTM on the adsorption capacity, 0.1 g MCTTM of different thickness were added into flasks, each of which contained 50 mL copper ions solution with an initial concentration of 20 mg L^{-1} at pH of 5–6. The ionic strength was controlled at 0.1 mol L^{-1} of $NaNO_3$. The mixture was stirred at 120 rpm at room temperature (20 °C) for 24 h.

2.4. Adsorption kinetic studies

Adsorption kinetic studies were carried out at different initial concentrations ranging from 10 mg L^{-1} to 25 mg L^{-1} in view of the results from previous work [18], viz. the adsorption amount increased with the increase of initial concentration. The container with 3 g MCTTM and 1.5 L copper ions solution was stirred at 120 rpm at room temperature (20 °C). And 5 mL samples were taken from the solution in a time intervals to analyze the copper ions concentration.

2.5. Arhenius activation energy

In order to examine the adsorption Arhenius activation energy of the adsorption of copper ions onto the MCTTM, a 0.1 g amount of the MCTTM was added into a number of flasks, each of which contained 50 mL of copper solution with an initial concentration of 20 mg L^{-1}, the initial pH of the solutions was adjusted at 5–6. The mixture was stirred in a shaker at 120 rpm at different temperatures of 298 K, 308 K and 318 K for 24 h.

Average and standard deviation values from triplicates were calculated using Microsoft Office XP. The figures and the coefficient (R^2) values of the non-linear form of kinetic models were determined using Matlab 7.0, and the other figures were obtained by Origin 7.5 and Chemoffice 2002.

2.6. Data processing

The amount of copper ions adsorbed on the MCTTM is calculated by:

$$q = \frac{(c_0 - c)V}{m} \quad (1)$$

The root mean square error, *RMSE* for each is derived from [20]:

$$RMSE = \sqrt{\frac{1}{m-2}\sum_{i=1}^{m}(Q_i - q_i)^2} \quad (2)$$

Dubinin–Radushkevich (D–R) isotherm model is used to estimate the adsorption free energy. It is shown in the following equation [21]:

$$Q = Q_{max}\ e^{\beta\varepsilon^2} \quad (3)$$

$$\varepsilon = RT_1\ \ln\left(1 + \frac{1}{C_e}\right) \quad (4)$$

The activity coefficient obtained from D–R isotherm model is suggested to be related to the adsorption free energy as [21]:

$$E = \frac{1}{\sqrt{-2\beta}} \quad (5)$$

The Arhenius equation is presented as follow [22]:

$$\ln\ k_2 = \ln\ k_0 - \frac{E_a}{RT} \quad (6)$$

The external mass transfer model describes the solute concentration change in the solution with time, and expresses as [23,24]:

$$\ln\ \frac{c_0 - c_s}{c - c_s} = k_f a_m t \quad (7)$$

The intra particle diffusion model of Vermeulen [21] investigated in this study is:

$$q = q_e\sqrt{1 - \exp\left(-\frac{\pi^3 k_V t}{36 q_e^2}\right)} \quad (8)$$

The intra particle diffusion model proposed by Weber and Morris is determined by the linear equation [25]:

$$q = C + k_{WM} t^{1/2} \quad (9)$$

The pseudo-first order kinetic model viz. Lagergren model is one of the most popular reaction kinetic models. For the liquid–solid adsorption system, it is summarized as follows [26]:

$$q = q_e\,(1 - e^{-k_1 t}) \quad (10)$$

The pseudo-second order equation is based on the sorption capacity on the solid phase. It deserves particular attention in present discussion because it predicts the behavior over the whole range of studies supporting a pseudo-second equation and bases on the assumption that chemisorption is the rate-controlling step [27,28].

It is assumed that the sorption capacity is proportional to the number of active sites occupied on the adsorbent:

$$q = \frac{q_e^2 k_2 t}{1 + q_e k_2 t} \quad (11)$$

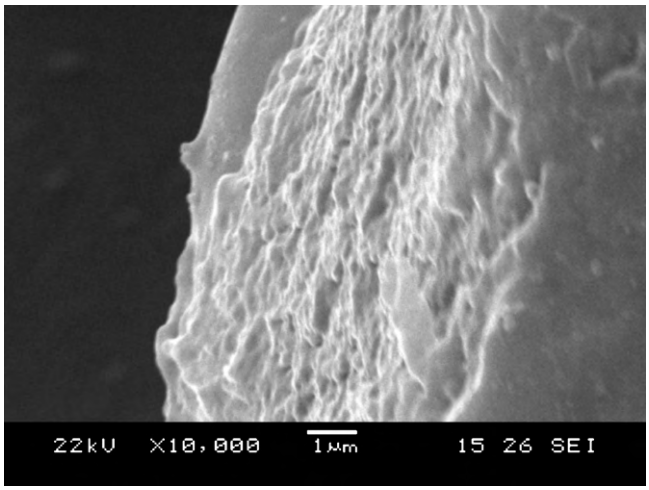

Fig. 1. SEM of the MCTTM cross-sectional image.

3. Results and discussion

3.1. Characteristics of the MCTTM

Fig. 1 shows the cross-sectional structure of the MCTTM obtained from the SEM analysis. The MCTTM is about 10 μm thick with a homogeneous structure. Some voids are visible at the cross section of the membrane, and there are lots of smaller porous voids appearing on the membrane surface.

FTIR spectra of the MCTTM were used for structural evaluations. The presence of a peak at a specific wavenumber indicates a specific chemical bond. Fig. 2 shows the FTIR spectra of the MCTTM before and after the adsorption process. The broad peaks at about 3290–3370 cm^{-1} which are concerned with –OH and –NH stretching vibrations decrease after adsorption process. The absorption peak at 1650 cm^{-1} (NH–$COCH_3$) and C=O stretching peak at about 1030–1070 cm^{-1} decrease, and the peak at about 1586 cm^{-1} for

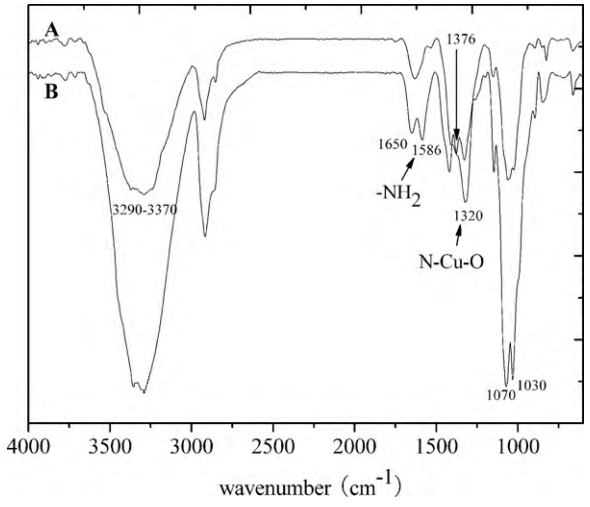

Fig. 2. FITR spectra of the MCTTM.

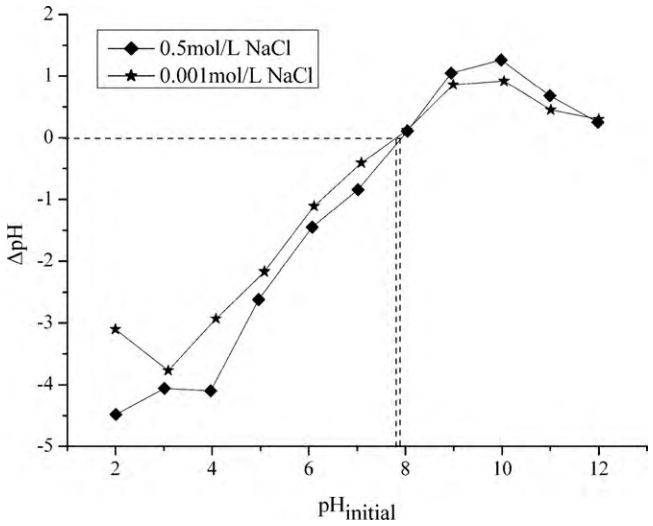

Fig. 3. The pH_{pzc} of the MCTTM.

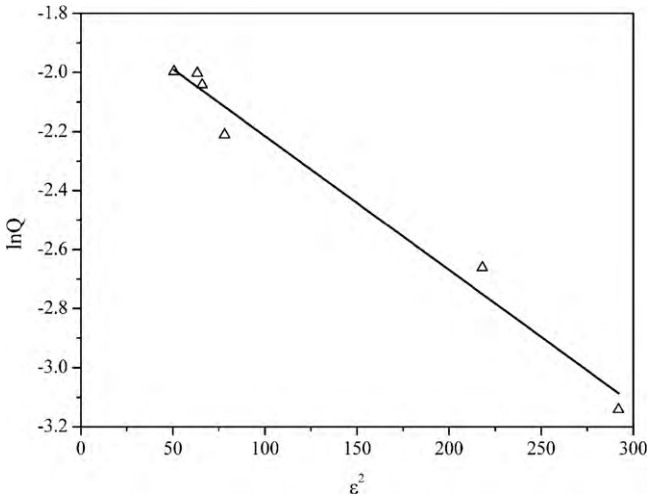

Fig. 5. The Dubinin–Radushkevich isotherm model.

$-NH_2$ group disappears while the peak at 1320 cm^{-1} which is concerned with N–Cu–O group appears and the absorption peaks at about 1376 cm^{-1} and 1419 cm^{-1} decrease.

Fig. 3 shows the ΔpH (pH_{final}–$pH_{initial}$) versus $pH_{initial}$ curves at different electrolyte concentrations and the pH_{pzc} of the MCTTM is about 7.8 as revealed by the point of $\Delta pH = 0$. There is a reasonable prediction that positively charged sites are predominant when pH is lower than 7.8, while negatively charged sites are predominant when pH is higher than 7.8.

3.2. Effect of membrane thickness

As discussed in our previous investigation, the solution pH obviously influenced the adsorption capacity of copper ions onto the MCTTM. The maximum removal efficiency of copper ions was about 92.9% at pH of 5–6 [18]. So the optimum pH 5–6 was chosen to investigate the effect of the membrane thickness. The results shown in Fig. 4 obviously indicate that the adsorption capacity decreases with the increase of the thickness of the MCTTM, which is due to less adsorption active sites distributed on the surface of the thicker MCTTM.

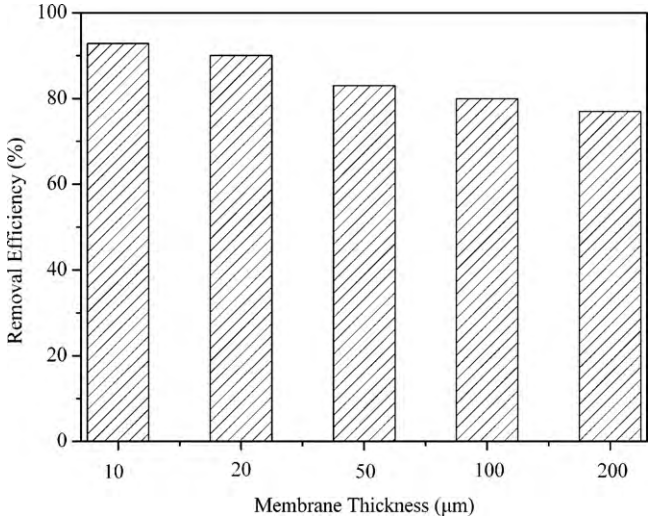

Fig. 4. The effect of the MCTTM thickness on the adsorption capacity.

3.3. Adsorption free energy

Fig. 5 illustrates the D–R isotherm model by plotting ln Q versus ε^2 according to the experimental data reported in Ref. [18]. The parameters, R^2, *RMSE* of Langmuir, Freundlich and D–R isotherm models and adsorption free energy (E) are presented in Table 2. It could be seen that the adsorption free energy E is 10.54 kJ mol^{-1}, which is within the energy range of ion exchange reactions, 8–16 kJ mol^{-1} [29]. A similar result about the ion exchange reaction process was reported by Oguz [30].

3.4. Adsorption kinetics

The kinetics provides valuable insights of the adsorption reaction mechanisms which involve mass transfer, diffusion and surface reaction phenomenon during the adsorption process [23,31]. The following mechanisms are considered to examine the adsorption kinetics of an adsorption process from which one or its probable combinations could be the rate-controlling mechanism(s):

(a) External mass transfer (boundary layer or film diffusion) between the external surface of the MCTTM and the surrounding fluid phase.
(b) Reaction on the external surface of the MCTTM.
(c) Intra particle diffusion, which may be limited by pore and solid diffusion.
(d) The chemical reaction on the activated sites of the intra-MCTTM.

Table 2
The parameters, R^2 and *RMSE* of Langmuir, Freundlich and D–R isotherm models and the adsorption free energy (E).

Langmuir	q_m	mg g^{-1}	8.414
	k_L	L mg^{-1}	0.1469
	R^2		0.9438
	RMSE		0.7318
Freundlich	k_F	(mg g^{-1})(L mg^{-1})	6.318
	n		3.930
	R^2		0.9620
	RMSE		0.6018
Dubinin-Radushkevich	Q_{max}	mol kg^{-1}	0.1719
	β	mol^2 kJ^2	−0.0045
	E	kJ mol^{-1}	10.54
	R^2		0.9742
	RMSE		0.0071

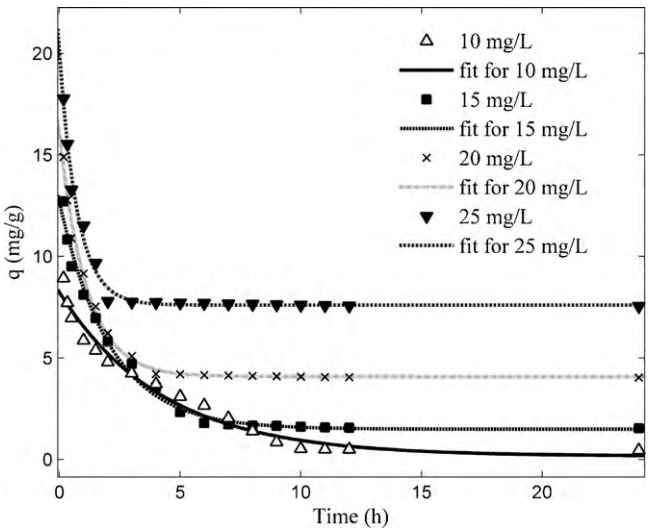

Fig. 6. External mass transfer model for the adsorption of copper ions on the MCTTM at four different concentrations of 10 mg L^{-1}, 15 mg L^{-1}, 20 mg L^{-1}, and 25 mg L^{-1}.

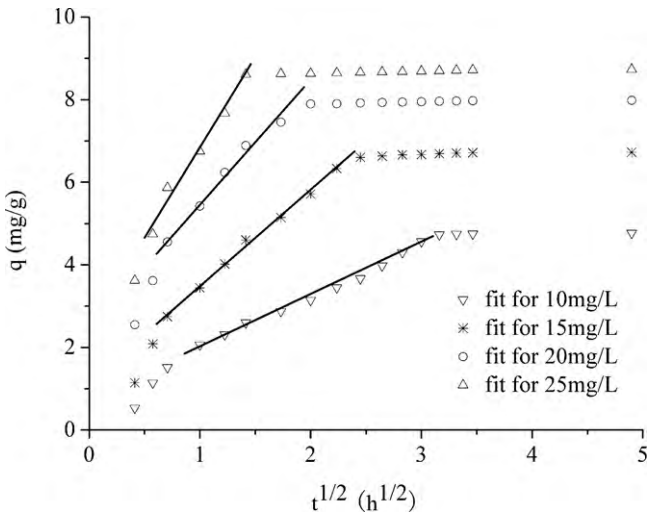

Fig. 7. Weber and Morris intra diffusion model for the adsorption of copper ions on the MCTTM at four different concentrations of 10 mg L^{-1}, 15 mg L^{-1}, 20 mg L^{-1}, and 25 mg L^{-1}.

Many attempts have been made to formulate a general expression describing the kinetics of adsorption on solid surfaces for liquid–solid phase systems [32–37] for which the proposed models could be classified in two groups namely the adsorption reaction and the diffusion models. Whilst the former include zero, first, second, third, pseudo-first and pseudo-second order, and the Langmuir–Hinshelwood and Elovich models. The latter contain external mass transfer and intra particle diffusion. By considering above mentioned mechanisms and the physical characters of the MCTTM showed in Table 1, the adsorptive performances of the MCTTM were delineated with reference to compatibility of results to the following diffusion and adsorption reaction models.

3.4.1. The application of diffusion kinetic models

3.4.1.1. External mass transfer model. Ho [27] reported that non-linear method could be a better way to obtain the kinetic parameters in the adsorption kinetics studies. The results of the non-linear regression analysis shown in Fig. 6 and Table 3 prove that copper ions adsorption on the MCTTM is well described by the external mass transfer model for all four of studied concentrations. The adsorption process quickly reaches equilibrium at higher initial copper ions concentration. This could be explained by the increased driving force in the liquid boundary layer surrounding the membrane. Ho et al. [28] reported that if film diffusion is rate-controlling step, the constant would vary inversely with the film thickness; while the constant would be independent of particle diameter and the flow rate, and would depend on the concentrations and the temperature if the exchange is chemically rate-controlling step. In addition, our investigations show that not only the membrane thickness (Fig. 4), but also the copper ions concentration and the temperature [18] could affect the rate constant. These results indicate that external mass transfer is a rate-controlling step in the diffusion process.

3.4.1.2. Intra particle diffusion model. Fig. 7 illustrates the Weber and Morris model at four different concentrations of copper ions. As seen from Fig. 7 and Table 3, the intra particle diffusion model of Vermeulen model, Weber and Morris model well described the experimental data. Weber and Morris [25] illustrated that if intra particle diffusion is the rate-controlling factor, adsorbate uptake

Table 3
The parameters, regression coefficients (R^2) and *RMSE* of kinetic models.

C_0 (mg L^{-1})		10	15	20	25
Pseudo-first order model	q (mg g^{-1})	4.549	6.589	7.815	8.587
	k_1 (h^{-1})	0.395	0.6915	1.496	2.295
	R^2	0.9405	0.9721	0.9713	0.9774
	RMSE	0.3867	0.3775	0.4083	0.3729
Pseudo-second order model	q (mg g^{-1})	5.263	7.347	8.363	9.041
	k_2 (g h mg^{-1})	0.09794	0.1317	0.2749	0.4098
	R^2	0.9697	0.9890	0.9940	0.9913
	RMSE	0.2758	0.2374	0.1862	0.232
Intra particle diffusion model of Vermeulen	q (mg g^{-1})	5.120	7.988	8.709	6.915
	k_V (mg $g^{-1})^2$ h^{-1}	0.07953	0.1111	0.1293	0.0849
	R^2	0.9861	0.9981	0.9962	0.9943
	RMSE	0.1868	0.1045	0.1533	0.1711
Intra particle diffusion model of Weber and Morris	C (mg g^{-1})	0.7214	1.256	2.554	1.973
	k_{WM} ($h^{-1/2}$)	1.252	2.237	2.927	4.794
	R^2	0.9937	0.9948	0.9843	0.9614
External mass transfer model	c_0 (mg L^{-1})	8.233	12.68	15.96	19.73
	c_s (mg L^{-1})	0.1732	1.498	4.085	7.628
	k_f (m h^{-1})	0.2343	0.4788	0.8837	1.267
	R^2	0.9704	0.9900	0.9934	0.9933
	RMSE	0.4733	0.4004	0.3028	0.2881

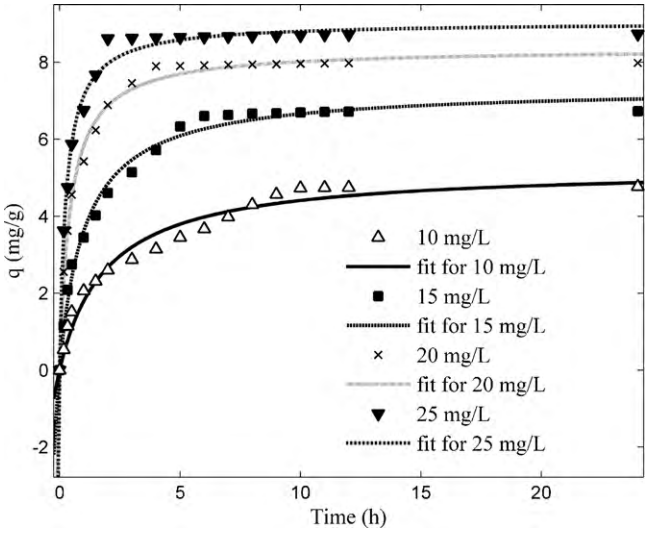

Fig. 8. Pseudo-second order model for the adsorption of copper ions on the MCTTM at four different concentrations of 10 mg L^{-1}, 15 mg L^{-1}, 20 mg L^{-1}, and 25 mg L^{-1}.

varies with the square root of time described by Eq. (8). In Fig. 7, the relation plot of q_t and $t^{1/2}$ does not go through the whole origin and three separated regions existed which indicates that intra particle diffusion is not the sole rate-controlling step [16] and three processes have taken place. A similar result was reported by Cheung et al. [38]. The linear portion describes a rapid adsorption stage on the external surface of the MCTTM. The plateau is attributed to the intra particle diffusion taking place after the completion of external surface coverage, the nature of the adsorption is concentration dependent so that chemical sorption is also a rate-controlling step via chelation ion exchange improved by the FTIR and adsorption free energy analysis.

Table 4
The parameters of the copper ions adsorption by the MCTTM.

Adsorbent	Temperature (K)	K_2 of pseudo-second order model (g h mg^{-1})	E_a (J mol^{-1})
The MCTTM	298	0.3044	679
	308	0.3068	
	318	0.3097	

3.4.2. The application of the reaction kinetic models

Fig. 8 represents the pseudo-second order model for the adsorption of copper ions onto the MCTTM at different concentrations. The parameters, R^2 and *RMSE* of the pseudo-first and pseudo-second order model are also shown in Table 3. As shown in Fig. 8 and Table 3, the pseudo-second order kinetic model fits the experimental data well. Though Table 3 shows the well description of the data by both pseudo-first and pseudo-second order models, as mentioned above, the nature of adsorption is a chemical-controlling

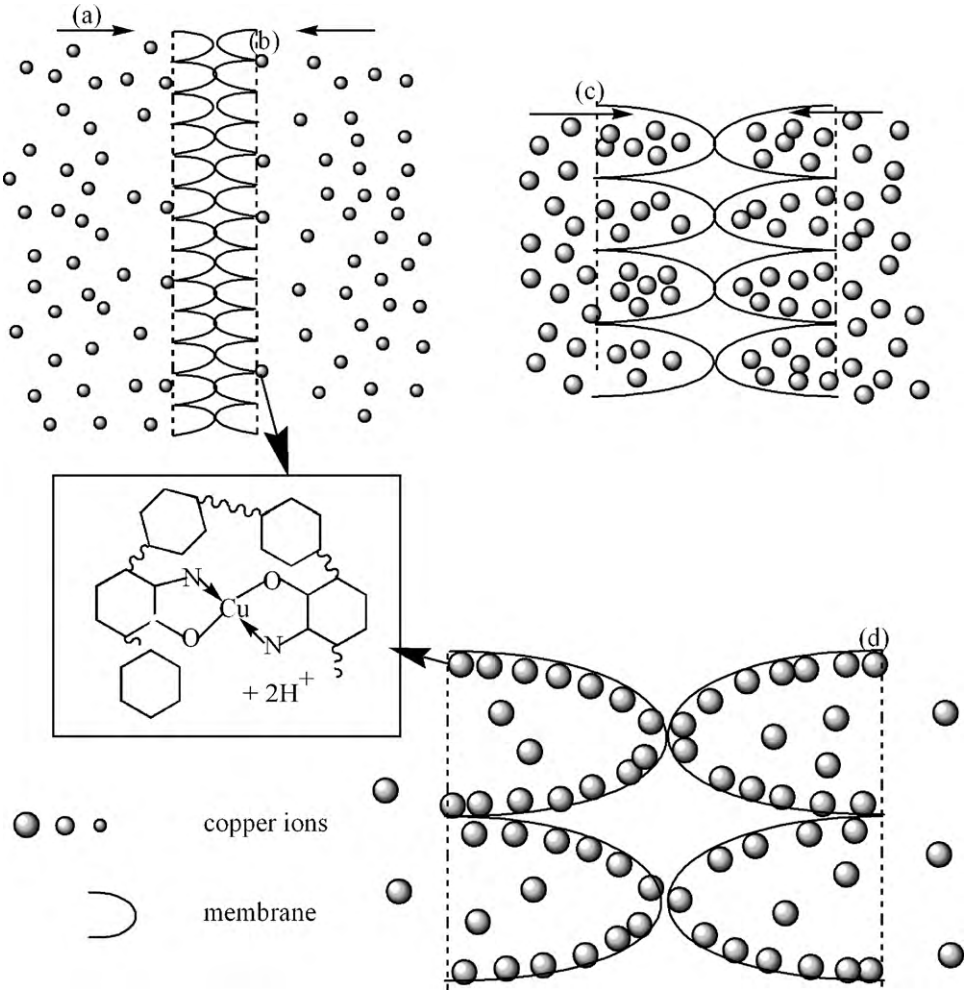

Fig. 9. Adsorption model: (a) external mass transfer process of copper ions from solution to the MCTTM; (b) reaction on the external surface of the MCTTM; (c) intra particle diffusion of copper ions within the particle of the MCTTM; (d) chemical reaction on the active sites inside of the MCTTM.

process. This is well compatible with the pseudo-second order model.

In order to evaluate the Arhenius activation energy of the adsorption process, pseudo-second order model was fitted the experimental data obtained from different temperatures of 298 K, 308 K and 318 K. Then the parameters k_2 of the model was used to calculate the Arhenius activation energy E_a.

The E_a could be calculated from the plot obtained from the ln k versus $1/T$. The result is presented in Table 4. The Arhenius activation energy is 679 J mol^{-1}.

3.5. Adsorption mechanism

The MCTTM has a good hydrophilic property with a WSR (water swelling ratio) of 126%. It could be explained by the alcohol groups in the chitosan which lead to higher degree of swelling because alcohol groups readily attract water molecules through hydrogen bonding. The good hydrophilic property makes the MCTTM exists steadily in the aqueous solution. In addition, Ho et al. [28] reported that acid groups on the sorbent could provide ion exchange sites for metal ions and ionic dyes; amine groups could provide a lone pair of electrons for chelating with metal ions; relatively insertion of sorbent surface may only provide physical sites for diffusional controlled bond formation. Beppu et al. [3] illustrated that the interaction between heavy metal ions and the chitosan included both chelating and ion exchange mechanism. Steenkamp et al. [39] reported that chitosan had chelation ion exchange properties which make use of the advantage of three dimensional structures of molecules to chelate and remove copper ions. From our investigation, the adsorption of copper ions onto the MCTTM includes chelation ion exchange process due to the existence of –NH_2 groups in the chitosan which is proved by the FTIR analysis and adsorption free energy analysis as well.

The optimal pH of solution for copper ions adsorption is 5–6 and Cu^{2+} is the only ionic species presented in the solution when pH is lower than 8.22 [40]. According to the study, the pH_{pzc} of the MCTTM is about 7.8 as shown in Fig. 3. When the solution pH is in the range of 5–6, the surface charge of the MCTTM is positive and it is unfavorable for electrostatic interaction between the MCTTM and copper ions. So it could be deduced that the copper ions are adsorbed on the MCTTM through an inner-sphere complex via surface chelation ion exchange rather than electrostatic interaction. The mechanism of adsorption of copper ions onto the MCTTM is described in Fig. 9.

4. Conclusions

A MCTTM is prepared by solution casting method from Chitosan. The SEM analysis indicates that the MCTTM is homogeneous porous structure which provides high specific surface and binding capacities for adsorption. The thickness of the MCTTM obviously affects the adsorption capacity of copper ions from solutions. The adsorption kinetics of copper ions onto the MCTTM is investigated in batch adsorption experiments and the results obtained from the experiments indicate that:

(i) The pseudo-second order model could describe the adsorption process, and the adsorption process is a chemical adsorption behavior of chelation ion exchange which can be proved by FTIR and adsorption free energy analysis.
(ii) Both external mass transfer and intra particle diffusion are the rate-controlling processes. At the very beginning of the adsorption process, the rate-controlling process is the external mass transfer process and then the intra particle mass diffusion process at the later time of process.
(iii) The adsorption free energy and the Arhenius activation energy of the adsorption process are 10.54 kJ mol^{-1} and 679 J mol^{-1}, respectively.

References

[1] G. Cimino, A. Passerini, G. Toscano, Removal of toxic cations and Cr(VI) from aqueous solutions by hazelnut shell, Water Res. 34 (2000) 2955–2962.
[2] W.S. Wan Ngah, M.A.K.M. Hanafiah, Removal of heavy metal ions from wastewater by chemically modified plant wastes as adsorbents: a review, Bioresour. Technol. 99 (2008) 3935–3948.
[3] M.M. Beppu, E.J. Arruda, R.S. Vieira, N.N. Santos, Adsorption of Cu (II) on porous chitosan membranes functionalized with histidine, J. Membr. Sci. 240 (2004) 227–235.
[4] X.F. Zeng, E. Ruckenstein, Supported chitosan-dye affinity membranes and their protein adsorption, J. Membr. Sci. 117 (1996) 271–278.
[5] B. Yu, Y. Zhang, A. Shukla, S.S. Shukla, K.L. Dorris, The removal of heavy metal from aqueous solutions by sawdust adsorption-removal of copper, J. Hazard. Mater. B80 (2000) 33–42.
[6] A. Nagendran, A. Vijayalakshmi, D.L. Arockiasamy, K.H. Shobana, D. Mohan, Toxic metal ion separation by cellulose acetate/sulfonated poly(ether imide) blend membranes: effect of polymer composition and additive, J. Hazard. Mater. 155 (2008) 477–485.
[7] C.J. Williams, D. Aderhold, R.G.J. Edyvean, Comparison between biosorbents for the removal of metal ions from aqueous solutions, Water Res. 32 (1998) 216–224.
[8] S.E. Bailey, T.J. Olin, R.M. Bricka, D.D. Adrian, A review of potentially low-cost sorbents for heavy metals, Water Res. 33 (1999) 2469–2479.
[9] C.X. Liu, R.B. Bai, Adsorptive removal of copper ions with highly porous chitosan/cellulose acetate blend hollow fiber membranes, J. Membr. Sci. 284 (2006) 313–322.
[10] Z.C. Feng, Z.Z. Shao, J.R. Yao, Y.F. Huang, X. Chen, Protein adsorption and separation with chitosan-based amphoteric membranes, Polymer 50 (2009) 1257–1263.
[11] G. Gibbs, J.M. Tobin, E. Guibal, Influence of chitosan preprotonation on reactive black 5 sorption isotherms and kinetics, Ind. Eng. Chem. Res. 43 (2004) 1–11.
[12] Z. Bekçi, C. Özveri, Y. Seki, K. Yurdakoç, Sorption of malachite green on chitosan bead, J. Hazard. Mater. 154 (2008) 254–261.
[13] H.L. Vasconcelos, T.P. Camargo, N.S. Gonçalves, A. Neves, M.C.M. Laranjeira, V.T. Fávere, Chitosan crosslinked with a metal complexing agent: synthesis, characterization and copper(II) ions adsorption, React Funct. Polym. 68 (2008) 572–579.
[14] W.S. Van Ngah, S. Fatinathan, Adsorption of Cu(II) ions in aqueous solution using chitosan beads, chitosan-GLA beads and chitosan-alginate beads, Chem. Eng. J. 143 (2008) 62–72.
[15] B. Kannamba, K.L. Reddy, B.V. AppaRao, Removal of Cu(II) from aqueous solutions using chemically modified chitosan, J. Hazard. Mater. 175 (2010) 939–948.
[16] S.R. Popuri, Y. Vijaya, V.M. Boddu, K. Abburi, Adsorptive removal of copper and nickel ions from water using chitosan coated PVC beads, Bioresour. Technol. 100 (2009) 194–199.
[17] L. Jin, R.B. Bai, Mechanisms of Lead adsorption on chitosan/PVA hydrogel beads, Langmuir 18 (2002) 9765–9770.
[18] X.S. Liu, Z.H. Cheng, W. Ma, Removal of copper by a modified chitosan adsorptive membrane, Front. Chem. Eng. China 3 (2009) 102–106.
[19] I.D. Smičiklas, S.K. Milonjić, P. Pfendt, S. Raičević, The point of zero charge and sorption of cadmium (II) and strontium (II) ions on synthetic hydroxyapatite, Sep. Purif. Technol. 18 (2000) 185–194.
[20] Z. Chen, W. Ma, M. Han, Biosorption of nickel and copper onto treated alga (*Undaria pinnatifida*): application of isotherm and kinetic models, J. Hazard. Mater. 155 (2008) 327–333.
[21] R. Apiratikul, P. Pacasant, Batch and column studies of biosorption of heavy metals by *Caulerpa Lentillifera*, Bioresour. Technol. 99 (2008) 2766–2777.
[22] S. Mustafa, K.H. Shah, A. Naeem, M. Waseem, M. Tahir, Chromium (III) removal by weak acid exchanger Amberlite IRC-50 (Na), J. Hazard. Mater. 160 (2008) 1–5.
[23] J.C. Shen, Z. Duvnjak, A reversible surface reaction model with an effectiveness factor and its application to sorption kinetics of cupric ions on corncob particles, Sep. Purif. Technol. 44 (2005) 69–77.
[24] G.M. Walker, L. Hansen, J.A. Hanna, S.J. Allen, Kinetics of a reactive dye adsorption onto dolomitic sorbents, Water Res. 37 (2003) 2081–2089.
[25] W.J. Weber, J.C. Morris, Kinetics of adsorption on carbon from solution, J. San. Eng. Div. 89 (1962) 31–39.
[26] Y.S. Ho, Citation review of Lagergren kinetic rate equation on adsorption reactions, Scientometrics 59 (2004) 171–177.
[27] Y.S. Ho, Second-order kinetic model for the sorption of cadmium onto tree fern: a comparison of linear and non-linear methods, Water Res. 40 (2006) 119–125.
[28] Y.S. Ho, J.C.Y. Ng, G. McKay, Kinetics of pollutant sorption by biosorbents: review, Sep. Purif. Methods 29 (2000) 189–232.
[29] W. Riemam, H. Walton, Ion exchange in analytical chemistry, in: International Series of Monographs in Analytical Chemistry, Pergamon Press, Oxford, 1970.
[30] E. Oguz, Equilibrium isotherms and kinetics studies for the sorption of fluoride on light weight concrete materials, Colloids Surf. A 295 (2007) 258–263.

[31] N.K. Lazaridis, D.D. Asouhidou, Kinetics of sorptive removal of chromium (VI) from aqueous solutions by calcined Mg–Al–CO_3 hydrotalcite, Water Res. 37 (2003) 2875–2882.
[32] Y.S. Al-Degs, M.I. El-Barghouthi, A.A. Issa, M.A. Khraisheh, G.M. Walker, Sorption of Zn(II), Pb(II), and Co(II) using natural sorbents: equilibrium and kinetic studies, Water Res. 40 (2006) 2645–2658.
[33] B. Yasemin, T. Zeki, Removal of heavy metals from aqueous solution by sawdust adsorption, J. Environ. Sci. 19 (2007) 160–166.
[34] A.L. Ahmad, S. Sumathi, B.H. Hameed, Adsorption of residue oil from palm oil mill effluent using powder and flake chitosan: equilibrium and kinetic studies, Water Res. 39 (2005) 2483–2494.
[35] N. Akhtar, M. Iqual, I.S. Zafar, J. Iqbal, Biosorption characteristics of unicellular green laga Chlorella sorokiniana immobilized in loofa sponge for removal of Cr(III), J. Environ. Sci. 20 (2008) 231–239.
[36] X.J. Wang, S.Q. Xia, L. Chen, J.F. Zhao, J.M. Chovelon, J.R. Nicole, Biosorption of cadmium(II) and lead(II) ions from aqueous solutions onto dried activated sludge, J. Environ. Sci. 18 (2006) 840–844.
[37] K. Akhtar, M.W. Akhtar, A.M. Khalid, Removal and recovery of uranium from aqueous solutions by Tichoderma harzianum, Water Res. 41 (2007) 1366–1378.
[38] W.H. Cheung, Y.S. Szeto, G. McKay, Intraparticle diffusion processes during acid dye adsorption onto chitosan, Bioresour. Technol. 98 (2007) 2897–2904.
[39] G.C. Steenkamp, K. Keizer, H.W.J.P. Neomagus, H.M. Krieg, Copper (II) removal from polluted water with alumina/chitosan composite membranes, J. Membr. Sci. 197 (2002) 147–156.
[40] J. Guzman, I. Saucedo, J. Revilla, R. Navarro, E. Guibal, Copper sorption by chitosan in the presence of citrate ions: influence of metal speciation on sorption mechanism and uptake capacities, Int. J. Biol. Macromol. 33 (2003) 57–65.